Alkyl Yttrium Complexes of Doubly Cyclometallated Xanthene- and Naphthalene-Backbone Bis(phosphinimine) Ligands

Aathith Vasanthakumar,[a] David J. H. Emslie,[a,*] and James F. Britten[b]

[a] *Department of Chemistry and Chemical Biology, McMaster University, 1280 Main Street West, Hamilton, Ontario, L8S 4M1, Canada*

[b] *McMaster Analytical X-Ray Diffraction Facility, 1280 Main Street West, Hamilton, Ontario, L8S 4M1, Canada*

Abstract

The synthesis of a rigid 4,5-bis(triphenylphosphinimino)-2,7-di-*tert*-butyl-9,9-dimethylxanthene {$(Ph_3PN)_2XT$} ligand is outlined, along with a modified synthesis for previously reported 1,8-bis(triphenylphosphinimino)naphthalene {$(Ph_3PN)_2NAP$}. Reaction of neutral $(Ph_3PN)_2XT$ with $[Y(CH_2SiMe_3)_3(THF)_2]$ resulted in double cyclometallation, yielding the base-free monoalkyl complex, $[(\{Ph_2(C_6H_4)PN_2XT)Y(CH_2SiMe_3)]$ (**1**). Layering a concentrated THF solution of **1** with hexanes at –28 °C afforded THF-coordinated $[(\{Ph_2(C_6H_4)PN\}_2XT)Y(CH_2SiMe_3)(THF)]\cdot 2THF$ (**1-THF**·2THF), with a distorted pentagonal pyramidal geometry and approximately meridional coordination of the pentadentate $\{Ph_2(C_6H_4)PN\}_2XT$ dianion. Similarly, $(Ph_3PN)_2NAP$ reacted with $[Y(CH_2SiMe_3)_3(THF)_2]$ to afford a THF-coordinated monoalkyl complex, $[\{(Ph_2(C_6H_4)PN)_2NAP\}Y(CH_2SiMe_3)(THF)]$ (**2-THF**). Layering a DME solution of **2-THF** with hexanes at –28 °C afforded X-ray quality crystals of $[[\{(Ph_2(C_6H_4)PN)_2NAP\}Y(CH_2SiMe_3)(\kappa^2\text{-DME})]\cdot$hexane (**2-DME**·hexane), with a highly distorted pentagonal pyramidal geometry and a facial coordination mode of the tetradentate $\{Ph_2(C_6H_4)PN\}_2NAP$ dianion.

1. Introduction

Group 3 and f-element alkyl and aryl complexes feature polar metal–carbon bonds, and demonstrate high reactivity of broad applicability in small molecule activation and catalysis. [1] Organometallic rare earth and actinide chemistry was originally dominated by complexes with carbocyclic supporting ligands, such as cyclopentadienyl anions. However, over the past several decades, rare earth non-cyclopentadienyl chemistry has experienced a surge of interest, due to the enormous steric and electronic variety offered by such ligands.[1] Our group has previously accessed a range of thermally robust rare earth, thorium and uranium organometallic complexes utilizing rigid dianionic 4,5-di(arylamido)-2,7-di-*tert*-butyl-9,9-dimethylxanthene pincer ligands (e.g. XA_2 and XN_2 in Figure 1). These complexes include neutral thorium(IV) and uranium(IV) alkyl complexes,[2, 3, 4] thorium(IV) monoalkyl cations,[3, 5] a thorium(IV) dication,[3] and neutral yttrium(III) or lutetium(III) monoalkyl complexes; the latter are extremely active for both intramolecular and intermolecular alkene hydroamination.[6, 7]

To further explore the applications of rigid pincer ligands in rare earth chemistry, we became interested in analogues of XA_2 and XN_2 with different overall charges, including neutral ligands where

both amido anions have been replaced with neutral N-donors (Figure 1). In order to provide a direct analogy, and maximize the rigidity of the metal coordination pocket, the nitrogen donor atoms must be attached directly at the 4- and 5-positions of the xanthene ligand backbone. Therefore, the use of tethered (i.e. not fused to the xanthene backbone) pyridine or related heterocyclic donors is precluded. Acyclic imines are another alternative but are prone to nucleophilic attack at the imine carbon. By contrast, phosphinimine donors are resistant to this mode of decomposition, so are the focus in this work.

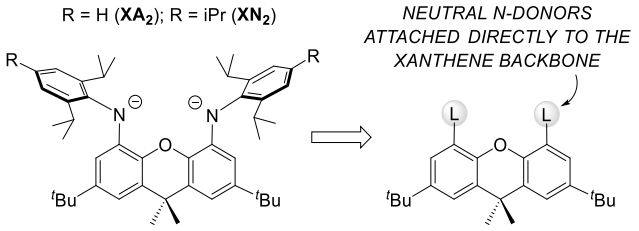

Figure 1. Dianionic XN_2 and XA_2 Ligands, and their relationship to the neutral NON-donor in this work.

A range of multidentate ligands incorporating phosphinimine donors have been deployed in rare earth hydrocarbyl chemistry over the past 15 years. For example, a series of monoanionic CGC (constrained geometry catalyst) ligands ('a' and 'b' in Figure 2) have been used to prepare both dialkyl and diaryl complexes. For ligand framework 'a',[8, 9] coordination occurred via both the phosphinimine donor and the cyclopentadienyl anion, with various hapticities observed for the latter. By contrast, with ligand 'b',[10] diaryl yttrium complexes, $[LY\{C_6H_4(CH_2NMe_2\text{-}o)\}_2]$, were isolated in which the supporting ligand coordinates only via the cyclopentadienyl ring, and not the extremely bulky phosphinimine donor. Ligand 'b' differs from the other ligands in Figure 2 in that the anionic donor is linked (within the backbone of the ligand) to the phosphinimine moiety via nitrogen, rather than phosphorus.

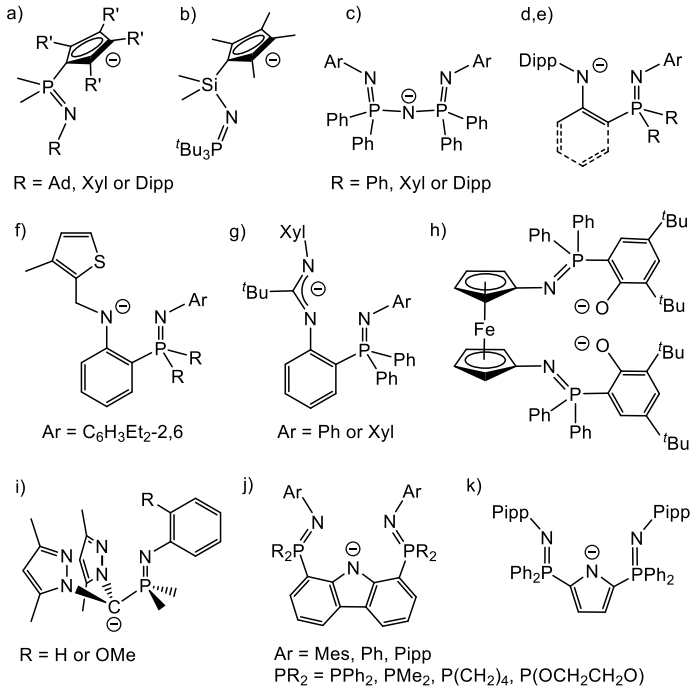

Figure 2. Phosphinimine-donor ligands employed in rare earth alkyl and aryl chemistry; for ligands 'd' and 'e', dashed bonds are absent in the former, and present in the latter (Ad = 1-adamantyl, Ar = aryl, Cy = cyclohexyl, Dipp = 2,6-diisopropylphenyl, Mes = mesityl, Pipp = *p*-isopropylphenyl, Xyl = 2,6-dimethylphenyl).

Ligands with an NPNPN framework ('c' in Figure 2)[11] and phosphinimine-containing analogues of β-diketiminate (nacnac) and anilido imine anions ('d'[12] and 'e'[13, 14] in Figure 2) have also been utilized for the synthesis of dialkyl rare earth complexes and a scandium alkyl cation. In dialkyl complexes of ligand 'd', cyclometallation appears to be promoted by increased ligand steric bulk; for example, in a series of $[LY(CH_2SiMe_3)_2(THF)_x]$ complexes, orthometallation of a *P*-phenyl ring was observed for Ar = $C_6H_3Et_2$-2,6, but not for Ar = Ph.[12] More complex ligands building from the anilido phosphinimine ligand framework have also been reported, including those with a pendant thiophene donor ('f' in Figure 2),[15] or where the amido donor has been replaced with an amidinate anion ('g' in Figure 2).[16] Furthermore, thermally unstable 5-coordinate $[LY(CH_2R)]$ (R = Ph or $SiMe_3$) complexes were prepared using a dianionic, tetradentate ligand in which a ferrocene backbone links two bidentate NO-donors; phosphinimine analogues of salicylaldiminate anions ('h' in Figure 2).[17]

Phosphinimine-containing heteroscorpionate ligands ('i' in Figure 2) have also been deployed for the synthesis of trivalent rare earth alkyl complexes,[18] as have tridentate ligands in which two phosphinimine donors are linked by an anionic carbazolide or pyrrolide backbone ('j' and 'k' in Figure 2). Ligand framework 'j' afforded dialkyl Sc, Y and Lu complexes which underwent rapid stepwise double cyclometallation.[19, 20-22] By contrast, dialkyl Sc, Lu, Er and Y complexes of ligand 'k' are stable for hours at 60 °C. However, switching to the larger Sm(III) ion resulted in rapid orthometallation of a phosphinimine *N*-aryl group, followed by orthometallation of a *P*-phenyl substituent. [23]

Herein we report the synthesis of a rigid 4,5-bis(triphenylphosphinimino)-2,7-di-*tert*-butyl-9,9-dimethylxanthene ligand, $(Ph_3PN)_2XT$, and yttrium alkyl complex synthesis via reaction with $[Y(CH_2SiMe_3)_3(THF)_2]$. Additionally, for the purpose for comparison, analogous reactivity was explored using the previously reported 1,8-bis(triphenylphosphinimino)naphthalene ligand, $(Ph_3PN)_2NAP$, which features a substantially smaller metal binding pocket.

2. Results and Discussion

2.1 Synthesis of the $(Ph_3PN)_2XT$ Ligand

The 4,5-dibromo-2,7-di-*tert*-butyl-9,9-dimethylxanthene precursor was dilithiated using 2 equiv. of ^{n}BuLi, and subsequent treatment with 2 equiv. of tosyl azide afforded the diazide species $(N_3)_2XT$. This intermediate was not isolated, but was reacted *in situ* with 2 equiv. of PPh_3 to afford $(Ph_3PN)_2XT$ (Scheme 1). The bright yellow $(Ph_3PN)_2XT$ ligand is moisture sensitive in solution, but is air- and water-stable as a solid. Solution NMR spectra for $(Ph_3PN)_2XT$ are consistent with the expected C_{2v}-symmetric structure; a single C*Me*$_2$ signal was observed by ^{1}H and ^{13}C NMR spectroscopy, and the ^{31}P NMR spectrum features a single peak at –1.95 ppm, with a similar chemical shift to other aryl phosphinimines. [20, 22] Furthermore, the empirical formula and purity of $(Ph_3PN)_2XT$ were confirmed through combustion elemental analysis.

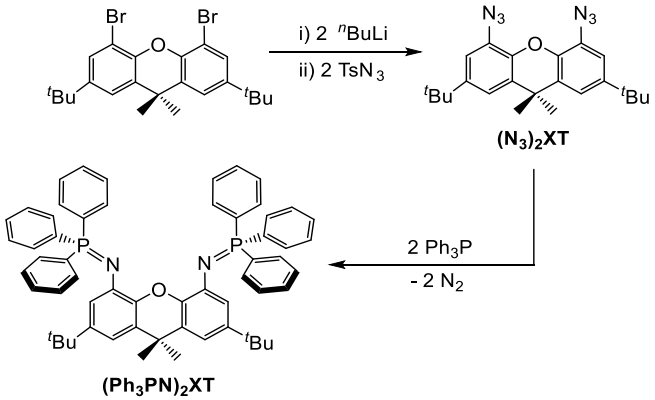

Scheme 1. One pot synthesis of the $(Ph_3PN)_2XT$ ligand utilizing the Staudinger reaction.

2.2 Synthesis of $[(\{Ph_2(C_6H_4)PN\}_2XT)Y(CH_2SiMe_3)]$

Reaction of $[Y(CH_2SiMe_3)_3(THF)_2]$ with one equiv. of $(Ph_3PN)_2XT$ in toluene resulted in rapid double cyclometallation, eliminating 2 equiv. of $SiMe_4$ (Scheme 2). This yielded the base-free monoalkyl complex $[(\{Ph_2(C_6H_4)PN\}_2XT)Y(CH_2SiMe_3)]$ (**1**), which was isolated as an analytically pure off-white solid. As noted in the introduction, cyclometallation of multidentate ligands containing neutral –N=PAr_3 donors has been reported for various rare earth complexes.

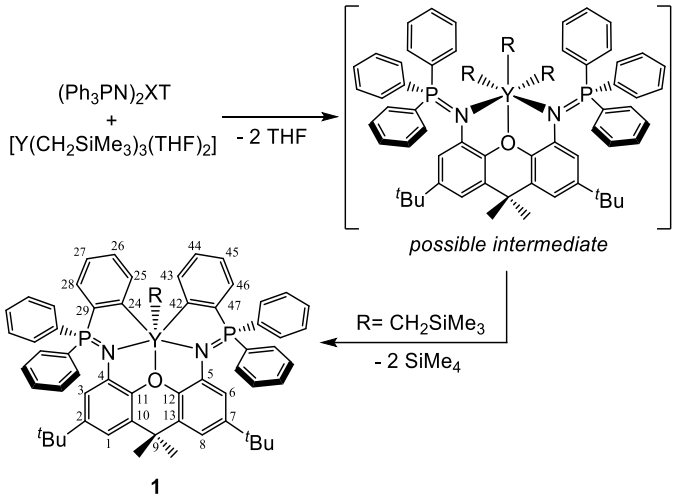

Scheme 2. Synthesis of [({$Ph_2(C_6H_4)PN$}$_2$XT)Y(CH_2SiMe_3)] (**1**).

In C_6D_6 or d_8-THF at room temperature, compound **1** appears C_s symmetric, resulting in two separate C*Me*$_2$ environments and a single ^{31}P NMR signal (28.85 ppm, d, $^3J_{Y,P}$ 11.4 Hz in C_6D_6), at a higher frequency than that of the free ligand. The original $(Ph_3PN)_2XT$ ligand has been cyclometallated at the *ortho* position of a phenyl ring on *each* of the two phosphorus centres, and these equivalent cyclometallated carbon atoms are significantly deshielded, giving rise to a ^{13}C NMR signal at δ 199.63 ppm. This chemical shift is comparable to that in other rare earth aryl complexes.[24] The Y*CH*$_2$ ^{1}H and ^{13}C NMR signals were observed at 0.19 and 34.68 ppm, respectively, with a $^1J_{C,H}$ coupling constant of 103 Hz, which is smaller than that for a typical sp^3 hydridized carbon atom ($^1J_{C,H}$ = 120-130 Hz), and is characteristic of an α-agostic interaction.[4,25]

Attempts to obtain X-ray quality crystals of base-free **1** were unsuccessful. However, layering a concentrated THF solution of **1** with hexanes at –28 °C afforded THF-coordinated [({$Ph_2(C_6H_4)PN$}$_2$XT)Y(CH_2SiMe_3)(THF)]·2THF (**1-THF**·2THF). This structure (Figure 4) confirmed that cyclometallation had occurred at the *ortho* position of a phenyl ring on each of the two phosphinimine donors, resulting in a series of four edge-sharing 5-membered metallacycles. The coordination geometry of **1-THF** is distorted pentagonal bipyramidal, with the κ^5-coordinated {$Ph_2(C_6H_4)PN$}$_2$XT ligand in the pentagonal plane, and THF and alkyl ligands in apical positions. Yttrium is located only 0.27 Å out of the N(1)/O(1)/N(2) plane, displaced in the direction of the alkyl ligand. The aryl donors are coordinated 0.40-0.69 Å above and below the plane of the nitrogen and oxygen atoms of the dianion, and the angle between the planes of the two cyclometallated aryl rings is 53°; this distortion likely occurs in order to minimize unfavorable steric interactions between the *meta*-C*H* protons on the two rings.

In complexes of related 4,5-bis(amido)xanthene ligands, the rigidity of the xanthene ligand backbone has been shown to be highly effective in ensuring approximately meridional coordination of the NON-donor array.[2, 3-5, 26] However, bending at the central non-aromatic ring can still be accommodated, and is most often observed upon coordination to small metal ions

such as magnesium(II) and aluminum(III).[7, 27] In the case of **1-THF**, the xanthene backbone is essentially planar, with an angle of just 3° between the planes of the two xanthene aryl rings.

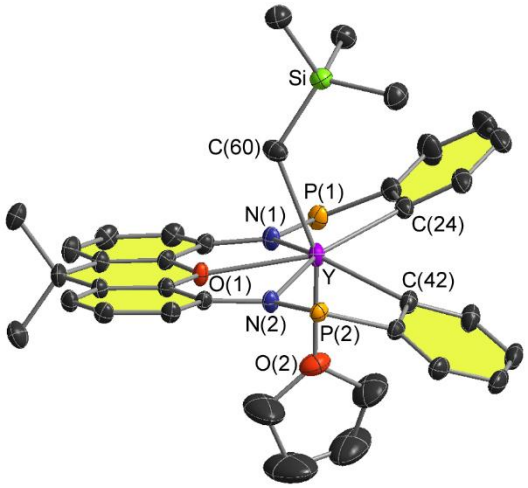

Figure 4. X-Ray crystal structure of [({$Ph_2(C_6H_4)PN$}$_2$XT)Y(CH_2SiMe_3)(THF)]·2THF (**1-THF**·2THF). Ellipsoids are set to 50% probability. For clarity, hydrogen atoms, lattice solvent, *tert*-butyl groups, and non-cyclometallated phenyl rings on phosphorus are omitted, and the xanthene backbone and cyclometallated phenyl rings of the {$Ph_2(C_6H_4)PN$}$_2$XT dianion are shaded in yellow. Selected bond lengths (Å) and angles (°): Y–C(60) 2.465(3), Y–C(24) 2.505(3), Y–C(42) 2.541(3), Y–N(1) 2.440(2), Y–N(2) 2.463(2), Y–O(1) 2.459(2), Y–O(2) 2.439(2), N(1)–P(1) 1.613(2), N(2)–P(2) 1.612(2), N(1)–Y–N(2) 131.31(7), Y–C(60)–Si 127.14(1), C(60)–Y–O(1) 79.21(8), C(60)–Y–O(2) 158.54(9).

The Y–C_{alkyl} distance of 2.465(3) Å falls at the high end of the range reported for neutral yttrium trimethylsilylmethyl complexes (which are more commonly 2.36 to 2.45 Å),[28] presumably due to the high coordination number in **1**. Other trimethylsilylmethyl complexes with similar Y–C distances include [{($Me_2N\{CH_2\}_2)_2N(CH_2)_2N^tBu$}Y($CH_2SiMe_3)_2$] (Y–C = 2.463(2) Å),[29] [{^{i}Pr$_2$TACN($SiMe_2$)N^{t}Bu}Y($CH_2SiMe_3)_2$] (Y–C = 2.465(4) Å; TACN = 1,4,7-triazacyclononane),[30] and [Cp*Y(CH_2SiMe_3){$CH(pz')_2$}(THF)] (Y–C = 2.462(2) Å; pz' = 3,5-dimethylpyrazolyl).[31] The Y–C(60)–Si bond angle in **1-THF** is 127.1(1)°, which is larger than typically observed for an sp^3 hybridized carbon atom. This is suggestive of an α-agostic interaction, consistent with the small $^1J_{C,H}$ NMR coupling constant measured for the Y*CH*$_2$ group of **1** in solution (*vide supra*). The Y–C_{aryl} bonds are 2.505(3) and 2.541(3) Å, again at the upper end of the usual range,[28] likely due to the high coordination number, combined with constraints associated with pentadentate coordination of the rigid ligand framework.

The P–N bond distances are 1.61(2) Å; similar to those in related group 3 phosphinimine complexes.[9, 13, 20] These P–N distances are slightly elongated in comparison to those in uncomplexed phosphinimine ligands, which typically range from 1.56 to 1.58 Å,[13, 20-22] suggesting some contribution from the zwitterionic resonance structure (with a positive charge on phosphorus and a negative charge on nitrogen). The Y–N bond distances {2.440(2) and 2.463(2)

Å} lie at the higher end of the range reported for yttrium phosphinimine complexes,[28] again likely due to the high coordination number in **1-THF**, combined with constraints imposed by the ligand framework. Similarly, the Y–O(1) distance to the xanthene backbone is 2.459(2) Å, which is longer than that in previously reported $[(XN_2)Y(CH_2SiMe_3)(THF)]\cdot O(SiMe_3)_2$ {$Y–O_{xant}$ = 2.347(2) Å},[7] which features the same xanthene backbone. The Y–O(2) bond to THF {2.439(2) Å} is only slightly shorter than Y–O(1), and falls within the usual range. [28]

2.3 Synthesis of the $(Ph_3PN)_2$NAP Ligand

Given that coordination of the $(Ph_3PN)_2XT$ ligand to yttrium resulted in rapid double cyclometallation to afford a κ^5-coordinated $Ph_2(C_6H_4)PN\}_2XT$ dianion (*vide supra*), we conjectured that a ligand backbone which reduces the distance between the phosphinimine donors (i.e. a ligand with a smaller metal binding pocket) may disfavor double cyclometallation, affording a mono-cyclometallated dialkyl yttrium complex. Therefore, the synthesis and complexation of an naphthalene-backbone bis-phosphinimine ligand, $(Ph_3PN)_2$NAP, was undertaken. This ligand was synthesized using a modified version of the literature preparation[32] (Scheme 3).

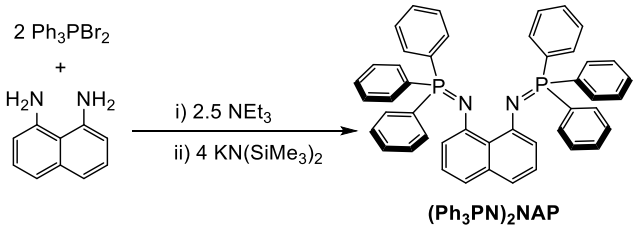

Scheme 3. Synthesis of the $(Ph_3PN)_2$NAP ligand using the Kirsanov reaction.

2.4 Synthesis of [({$Ph_2(C_6H_4)PN\}_2$NAP)$Y(CH_2SiMe_3)(THF)$] (2-THF)

Similar to the reactivity of $[Y(CH_2SiMe_3)_3(THF)_2]$ with $(Ph_3PN)_2XT$, reaction of $[Y(CH_2SiMe_3)_3(THF)_2]$ with 1 equiv. of $(Ph_3PN)_2$NAP afforded a doubly cyclometallated monoalkyl yttrium complex, [({$Ph_2(C_6H_4)PN\}_2$NAP)$Y(CH_2SiMe_3)(THF)$] (**2-THF**; Scheme 4). However, unlike base-free **1**, THF could not be removed from **2-THF** in vacuo at room temperature. Furthermore, **2-THF** decomposed to unidentified products at room temperature; over several hours in solution, and several days in the solid state. Room temperature NMR spectra of compound **2-THF** are indicative of C_s symmetry, with a single ^{31}P NMR signal at 28.49 ppm (d, $^2J_{89Y,31P}$ 12 Hz), and two sets of peaks for the intact phenyl rings on phosphorus. Again, cyclometallation was found to have occurred at the *ortho* position of a phenyl ring on each of the two phosphinimine donors, and the ^{13}C NMR chemical shift for the cyclometallated carbon was 197.52 ppm. The YCH_2 ^{1}H and ^{13}C NMR signals were located at –0.15 and 30.82 ppm, respectively, with a small $^1J_{C,H}$ coupling constant of 102 Hz (nearly identical to that in **1**), indicative of an α-agostic interaction.[4,25]

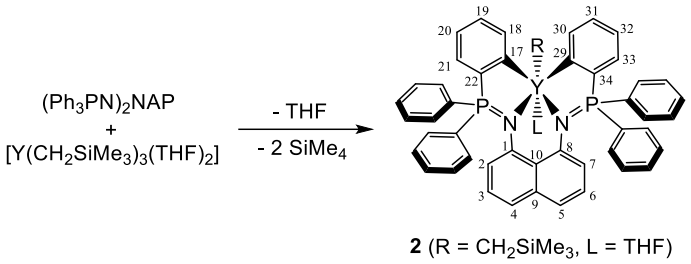

Scheme 4. Synthesis of [({$Ph_2(C_6H_4)PN$}$_2$NAP)Y(CH_2SiMe_3)(THF)] (**2-THF**)

X-ray quality crystals of **2-THF** proved elusive. However, crystals of [{($Ph_2(C_6H_4)PN)_2$NAP}Y(CH_2SiMe_3)(κ^2-DME)]·hexane (**2-DME**·hexane) were obtained from DME/hexanes at –28 °C. Complex **2-DME** is 7-coordinate (Figure 5), and can be described as a highly distorted pentagonal bipyramid, with the alkyl ligand and one of the aryl groups [C(29)] in axial sites. However, unlike the structure of **1-THF**, yttrium lies 1.53 Å out of the N(1)/C(9)/N(2) plane (cf. 0.27 Å out of the N(1)/O(1)/N(2) plane in **1-THF**). Effectively, the tetradentate ($Ph_2(C_6H_4)PN)_2$NAP dianion adopts a facial coordination mode, whereas the pentadentate ($Ph_2(C_6H_4)PN)_2$XT ligand coordinates meridionally.

The Y–C_{aryl} bonds in **2-DME** are 2.508(2) Å [Y–C(17)] and 2.562(2) Å [Y–C(29)], giving an average Y–C_{aryl} distance which is nearly identical to that in compound **1-THF**. By contrast, the Y–C(47) distance is 2.520(2) Å, which is even longer than the corresponding Y–C_{alkyl} distance in **1-THF** {2.465(3) Å}. This can be attributed to the high *trans* influence of the aryl group in the opposing axial site {C(47)–Y–C(29) = 161.70(8)°}, possibly combined with increased steric hindrance resulting from the smaller binding pocket and differently-placed steric bulk of the naphthalene-backbone ligand. The Y–C(47)–Si angle is also notably obtuse, at 139.2(1)°, indicative of an α-agostic interaction, in keeping with the solution NMR data for **2-THF** (*vide supra*). However, given that the $^1J_{C,H}$ NMR coupling constants for the YCH_2 groups in **1** and **2-THF** are nearly identical, the significantly more obtuse Y–C–Si angle in **2-DME** {cf. 127.1(1)° in **1-THF**} is also suggestive of appreciable steric hindrance. Moreover, steric hindrance is likely responsible for the long Y–O_{DME} distances of 2.493(2) and 2.534(2) Å in **2-DME** {cf. 2.439(2) Å for the Y–O_{THF} bond in **1-THF**}.

The P-N bonds are 1.613(2) and 1.632(2) Å, comparable to those in compound **1-THF**. However, the Y–N(1) and Y–N(2) distances are 2.518(2) and 2.401(2)Å; both longer and shorter than those in **1-THF** {2.440(2) and 2.463(2) Å}. The substantial difference between the Y–N distances in **2-DME** presumably stems from constraints imposed by the ligand framework, which enforces a non-ideal orientation of the lone pair on N(1) relative to yttrium {Y lies 0.59 Å out of the P(1)/N(1)/C(1) plane, compared to 0.03 Å out of the P(2)/N(2)/C(8) plane}.

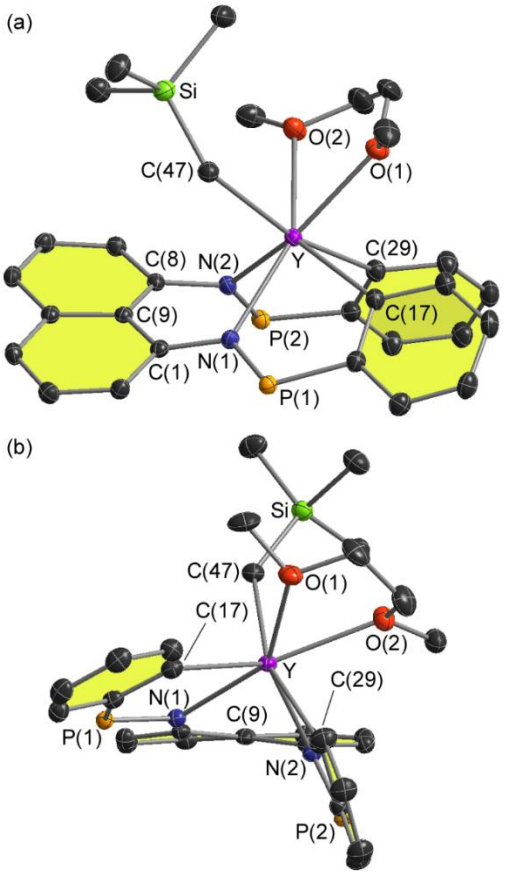

Figure 5. Two views of the X-ray crystal structure of [({$Ph_2(C_6H_4)PN$}$_2$NAP)Y(CH_2SiMe_3)(DME)]·hexane (**2-DME**·hexane). Ellipsoids are set to 50% probability. For clarity, hydrogen atoms, lattice solvent, and non-cyclometallated phenyl rings on phosphorus are omitted, and the naphthalene backbone and cyclometallated phenyl rings of the {$Ph_2(C_6H_4)PN$}$_2$NAP dianion are shaded in yellow. Selected bond lengths (Å) and angles (°): Y–C(47) 2.520(2), Y–C(17) 2.508(2), Y–C(29) 2.562(2), Y–N(1) 2.518(2), Y–N(2) 2.401(2), Y–O(1) 2.493(2), Y–O(2) 2.534(2), N(1)–P(1) 1.632(1), N(2)–P(2) 1.613(2), N(1)–Y–N(2) 70.69(6), Y–C(47)–Si 139.18(1), C(29)–Y–C(47) 161.70(8), C(17)–Y–C(47) 111.12(8).

Due to a coordination number of 6 at yttrium, neither **1** nor **2-THF** is active for ethylene polymerization (20 °C, 1 atm). Furthermore, addition of hydroamination substrates resulted in protonation of the aryl anions in the cyclometallated ligands and release of free ($Ph_3PN)_2$XT or ($Ph_3PN)_2$NAP. However, to the best of our knowledge, **1** and **2-THF** are the first isolated examples of monometallic rare earth alkyl diaryl complexes.[33]

3. Summary and Conclusions

The rigid xanthene-backbone bis(phosphinimine) ligand, ($Ph_3PN)_2$XT, was synthesized in 2 steps (one pot) from 4,5-dibromo-2,7-di-*tert*-butyl-9,9-dimethylxanthene, and a modified synthesis is

provided for the $(Ph_3PN)_2NAP$ ligand. Both bis(phosphinimine) ligands reacted with $[Y(CH_2SiMe_3)_3(THF)_2]$ to afford doubly cyclometallated monoalkyl yttrium complexes, $[(\{Ph_2(C_6H_4)PN\}_2XT)Y(CH_2SiMe_3)]$ (**1**) and $[(\{Ph_2(C_6H_4)PN\}_2NAP)Y(CH_2SiMe_3)(THF)]$ (**2-THF**). Compound **1** is thermally stable at room temperature, whereas **2-THF** slowly decomposed in solution and in the solid state. Crystals of 7-coordinate **1-THF** and **2-DME** were obtained from THF/hexanes and DME/hexanes, respectively. The geometry of **1-THF** is approximately pentagonal bipyramidal, with the pentadentate $(Ph_2(C_6H_4)PN)_2XT$ dianion coordinating meridionally. By contrast, the $(Ph_2(C_6H_4)PN)_2NAP$ dianion in **2-DME** adopts a facial coordination mode, resulting in a very different steric environment at the metal, and different co-ligand placement. These differences in coordination mode presumably stem from changes in the distance between the nitrogen atom attachment points on the ligand backbone (4.75 Å in $Ph_2(C_6H_4)PN\}_2XT$ vs 2.59 Å in $Ph_2(C_6H_4)PN\}_2NAP$), with the shorter distance preventing meridional coordination of the N- and C-donor atoms (due to a binding pocket of insufficient size).

4. Experimental

4.1 General Details

An argon-filled M-Braun UNIlab glovebox equipped with a –28°C freezer was employed for the manipulation and storage of all air sensitive compounds, and reactions were performed on a double manifold high vacuum line using standard techniques. A Fisher Scientific Ultrasonic FS-30 bath was used to sonicate reaction mixtures where indicated. Yttrium compounds reported in this article are very air and moisture sensitive, and the vacuum line operated at <5 mTorr. The argon stream was further purified using an Oxisorb-W scrubber from Matheson Gas Products. THF, hexanes, pentane and DME were initially dried and distilled at atmospheric pressure from Na/Ph_2CO. Toluene was initially dried and distilled at atmospheric pressure from Na. Unless otherwise indicated, all protio solvents were stored over an appropriate drying agent [pentane, hexanes, toluene: Na/Ph_2CO/tetraglyme] and vacuum distilled into reaction flasks or storage flasks for use within a glovebox. Deuterated solvents were purchased from Cambridge Isotope Laboratories. C_6D_6 was dried over Na/Ph_2CO/tetraglyme, and CD_2Cl_2 was dried over 4Å molecular sieves, prior to vacuum distillation to a storage flask.

4,5-dibromo-2,7-di-*tert*-butyl-9,9-dimethylxanthene,[34] $[Y(CH_2SiMe_3)_3(THF)_2]$,[35] and Tosyl Azide[36] were synthesized using literature procedures. $LiCH_2SiMe_3$ (1.0M in pentane), *n*BuLi (1.6M in hexanes), Br_2, Tosyl Chloride, *N*-benzylbenzamide, Ph_3PBr_2, 1,8-diaminonaphthalene, $KN(SiMe_3)_2$ and anhydrous YCl_3 were purchased from Sigma Aldrich. Sodium azide was purchased from J.T Baker Chemical Company. *n*BuLi was titrated according to a literature procedure.[37] $YCl_3(THF)_{3.5}$ was obtained by refluxing anhydrous YCl_3 in dry THF for 24 hours, followed by removal of solvent under vacuum. Argon (99.999%) was purchased from Praxair.

Combustion elemental analyses were performed by Midwest Microlab, LLC, Indianapolis, Indiana. NMR spectroscopy [^1H, $^{13}C\{^1H\}$, $^{31}P\{^1H\}$, DEPT-Q, COSY, HSQC, HMBC] was performed on a ruker AV-600 Spectrometer. All ^1H NMR and ^{13}C NMR spectra were referenced relative to $SiMe_4$ using the resonance of the deuterated solvent (^{13}C NMR) or protio impurity in

the deuterated solvent (^{1}H NMR); in ^{1}H NMR, 7.16 ppm for C_6D_6, 3.58 and 1.72 ppm for d_8-THF, and 5.32 ppm for CD_2Cl_2; in ^{13}C NMR, 128.06 ppm for C_6D_6, and 53.84 ppm for CD_2Cl_2. $^{31}P\{^1H\}$ NMR spectra were referenced using an external standard of 85 % H_3PO_4 in D_2O (δ 0.0 ppm). Compound numbering used for NMR assignment is shown in Schemes 2 and 4. X-ray crystallographic analyses were performed on suitable crystals coated in Paratone oil and mounted on a SMART APEX II diffractometer with a 3 kW Sealed tube Mo generator in the McMaster Analytical X-ray (MAX) Diffraction Facility. In all cases, non-hydrogen atoms were refined anisotropically and H atoms were generated in ideal positions and updated with each cycle of refinement.

X-ray crystallographic analysis were performed on suitable crystals coated in Paratone oil and mounted on a SMART APEX II diffractometer with a 3 kW Sealed tube Mo generator in the McMaster Analytical X-ray Diffraction Facility. The crystals were kept at 100.0(1) K during data collection. Using Olex2 [38], the structure was solved with the ShelXT [39] structure solution program using Intrinsic Phasing and refined with the ShelXL [40] refinement package using Least Squares minimisation.

For compound **1-THF**·2THF the *tert*-butyl groups were rotationally disordered over two positions. This was modelled and the occupancy was allowed to refine freely. An EADP command was used to constrain the thermal displacement parameters of the *t*-butyl groups of **1-THF**·2THF. **Crystal Data** for **1-THF**·2THF: monoclinic, space group $P2_1/c$ (no. 14), a = 18.2514(6) Å, b = 25.2101(8) Å, c = 14.8822(4) Å, β = 96.622(2)°, V = 6801.9(4) Å^3, Z = 4, T = 100.0(1) K, μ(MoKα) = 0.971 mm^{-1}, D_{calc} = 1.234 g/cm^3, 154430 reflections measured (2.246° ≤ 2Θ ≤ 61.154°), 20852 unique (R_{int} = 0.0598, R_{sigma} = 0.0422) which were used in all calculations. The final R_1 was 0.0613 (I > 2σ(I)) and wR_2 was 0.1646 (all data).

For **2-DME**·hexane, one molecule of hexane in the asymmetric unit is positionally disordered over two positions. This was modelled and the occupancy was allowed to refine freely. An EADP command was used to constrain the thermal displacement parameters of positionally displaced atoms of hexane. Crystal Data for **2-DME**·hexane: triclinic, space group P-1 (no. 2), a = 12.0075(10) Å, b = 12.3367(11) Å, c = 17.8701(15) Å, α = 85.720(5)°, β = 86.015(5)°, γ = 85.014(5)°, V = 2624.5(4) Å^3, Z = 2, T = 100.0(1) K, μ(MoKα) = 1.240 mm^{-1}, D_{calc} = 1.302 g/cm^3, 102199 reflections measured (2.29° ≤ 2Θ ≤ 60.644°), 15659 unique (R_{int} = 0.0713, R_{sigma} = 0.0615) which were used in all calculations. The final R_1 was 0.0475 (I > 2σ(I)) and wR_2 was 0.1149 (all data).

4.2 Synthesis of $(Ph_3PN)_2XT$: A 1.6 M solution of *n*BuLi in hexanes (1.02 mL, 1.66mmol) was added under a stream of argon to a solution of 4,5-dibromo-2,7-di-*tert*-butyl-9,9-dimethylxanthene (400mg, 0.83 mmol) in 50 mL of THF at –78 °C, and the reaction was stirred for 2 hours. A solution of tosyl azide (328 mg, 1.66 mmol) in approximately 2 mL of THF was added dropwise to the reaction at –78 °C, which was then allowed to warm to room temperature, and stirred for 24 h. A solution of PPh_3 (437 mg, 1.66 mmol) in approximately 5 mL of THF was added to the reaction at room temperature and the reaction was stirred for a further 24 h. Solvent was then evaporated in vacuo to afford a brown-yellow residue, which was purified in air; ~20 mL of Et_2O was added, followed by sonication, filtration, and washing of the solid with water (2 × ~20 mL), Et_2O (3 × ~10

mL), and hexanes (2 × ~20 mL). The solid was dried under vacuum at 45 °C for 16 hours, yielding $(Ph_3PN)_2XT$ as a bright yellow powder (523 mg, 72%). This ligand is moisture sensitive in solution, but air- and water-stable as a solid. **^{1}H NMR (C_6D_6, 600 MHz, 298K):** δ 8.02-7.99 (m, 12H, *o*-phenyl), 7.08 (dd, 2H, $^4J_{H,H}$ 2 Hz, $J_{P,H}$ 1 Hz, C$H^{1,8}$), 6.98-6.96 (m, 6H, *p*-phenyl), 6.88-6.85 (m, 12H, *m*-phenyl), 6.56 (appt. t, 2H, $^4J_{H,H}$ 2 Hz, $^4J_{P,H}$ 2 Hz, C$H^{3,6}$), 1.87 (s, 6H, CMe_2), 1.22 (s, 18H, CMe_3) ppm. **^{13}C{^{1}H} NMR (C_6D_6, 151 MHz, 298K):** δ 144.74 (d, $^2J_{P,C}$ 18 Hz, $C^{4,5}$), 143.16 (s, $C^{2,7}$), 139.37 (s, $C^{11,12}$), 133.59 (d, $^2J_{P,C}$ 9 Hz, *o*-Ph), 132.87 (s, *ipso*-Ph), 131.00 (s, *p*-Ph), 129.99 (s, $C^{10,13}$), 128.39 (d, $^3J_{P,C}$ 12 Hz, *m*-Ph), 118.80 (d, $^3J_{P,C}$ 9 Hz, CH^{3,6}), 111.93 (s, CH^{1,8}), 35.66 (s, CMe$_2$), 34.32 (s, CMe$_3$), 33.54 (s, CMe_2), 31.91 (s, CMe_3) ppm. **^{31}P{^{1}H} NMR (C_6D_6, 243 MHz, 298K):** δ –1.95 (s) ppm. **$C_{59}H_{58}O_1N_2P_2$ (873.05 g mol^{-1}):** calcd. C 81.17, H 6.70, 3.21 %; found C 80.95, H 6.82, N 3.05 %.

4.3 Synthesis of $(Ph_3PN)_2$NAP: A 100 mL round bottom flask was loaded with 1,8-diaminonaphthalene (100 mg, 0.63 mmol) and Ph_3PBr_2 (533 mg, 1.26 mmol), and ~50 mL of CH_2Cl_2 was condensed into the flask at –78 °C. Excess Et_3N (1 mL, 7.16 mmol) was added to the reaction at –78 °C, and the reaction mixture was allowed to warm up to room temperature. After stirring for 1 hour, solvent was removed in vacuo, and ~50 mL of THF was condensed into the flask, followed by sonication to suspend all the solid. The reaction was cooled to –45°C, and a solution of $KN(SiMe_3)_2$ (502 mg, 2.52 mmol) in 10 mL of THF was added slowly. The reaction was then brought to room temperature, and stirred for 1 hour prior to removal of solvent in vacuo to afford a bright yellow solid. This solid was purified in air; ~20 mL of Et_2O was added to the flask, followed by sonication to suspend the yellow solid, filtration, and washing of the solid with water (~20 mL), Et_2O (2 × ~20 mL), and then hexanes (2 × ~20 mL). Bright yellow $(Ph_3PN)_2$NAP was then dried at 45 °C in vacuo for 16 hours (351 mg, 82%). **^{1}H NMR (CD_2Cl_2, 600 MHz, 298K):** δ 7.95-7.92 (m, 12 H, *o*-Ph) , 7.41-7.39 (m, 6H, *p*-Ph), 7.23-7.20 (m, 12H, *m*-Ph), 6.85 (d, 2H, $^3J_{H,H}$ 8 Hz, C$H^{4,5}$), 6.73 (appt. t, 2H, $^3J_{H,H}$ 8 Hz, C$H^{3,6}$), 6.25 (d, $^3J_{H,H}$ 8 Hz, C$H^{2,7}$) ppm. **^{13}C{^{1}H} NMR (CD_2Cl_2, 151 MHz, 298K):** δ 150.52 (s, $C^{1,8}$), 138.91 (s, C^9), 133.52 (d, $^2J_{P,C}$ 10 Hz, *o*-Ph). 132.64 (s, *ipso*-Ph), 131.99 (s, C^{10}), 131.51 (s, *p*-Ph), 128.54(d, $^3J_{P,C}$ 12 Hz, *m*-Ph), 125.24 (s, CH^{3,6}), 116.95 (s, CH^{4,5}), 116.17 (d, $^3J_{P,C}$ 14 Hz, $C^{2,7}$). **^{31}P{^{1}H} NMR (CD_2Cl_2, 243 MHz, 298K):** δ –3.39 ppm. **$C_{46}H_{36}N_2P_2$ (678.74 g mol^{-1}):** calcd. C 81.40, H 5.35, N 4.13 %; found. C 81.18, H 5.61, N 4.06 %.

4.4 Synthesis of [({$Ph_2(C_6H_4)$PN}$_2$XT)Y(CH_2SiMe_3)] (1): A solution of $(Ph_3PN)_2XT$ (160 mg, 0.18 mmol) in toluene (15 mL) was added dropwise to a solution of $[Y(CH_2SiMe_3)_3(THF)_2]$ (100 mg, 0.20 mmol) in toluene (10 mL) at room temperature. The reaction was stirred for 1 hour and then the solvent was removed in vacuo to afford an off white solid. This solid was redissolved in 25 mL of toluene and the solvent was again removed in vacuo, in order to remove residual THF. This solid was washed with hexanes (3 × ~2 mL) and then dried under vacuum for 4 hours, yielding **1** as a highly air-sensitive off-white solid (128 mg, 68%). **^{1}H NMR (C_6D_6, 600 MHz, 298K):** δ 8.30 (d, 2H, $^3J_{H,H}$ 7 Hz , C$H^{25,43}$), 8.08-8.04 (m, 4H, *o*-Ph), 7.74-7.70 (m, 4H, *o*-Ph), 7.21-7.18 (m, 2H, C$H^{26,44}$), 7.17-7.15 (m, 2H, C$H^{28,46}$), 7.12-7.08 (m, 4H, *m*-Ph), 7.07-7.03 (m, 2H, *p*-Ph), 6.99-6.96 (m, 2H, C$H^{27,45}$), 6.93 (d, 2H, $^4J_{H,H}$ 2 Hz , C$H^{1,8}$), 6.92-6.90 (m, 2H, *p*-Ph), 6.86-6.83 (m, 4H, *m*-Ph), 6.83 (d, 2H, $^4J_{H,H}$ 2 Hz , C$H^{3,6}$) 1.71, 1.69 (s, 2 x 3H, CMe_2), 1.04 (s, 18H, CMe_3), 0.20 (s, 9H, CH_2SiMe_3), 0.19 (d, 2H, $^2J_{H,Y}$ 3 Hz, CH_2SiMe_3) ppm. **^{13}C{^{1}H} NMR (C_6D_6, 151**

MHz, 298K): δ 199.63 (dd, $^{1}J_{Y,C,}$ $^{2}J_{P,C}$ 44 Hz, 38 Hz, $C^{24,42}$), 146.14 (s, $C^{2,7}$), 143.82 (d, $^{2}J_{Y,C}$ 18 Hz, $C^{11,12}$), 142.34 (d, $^{2}J_{Y,C}$ 26 Hz, $CH^{25,43}$), 140.21 (s, *ipso*-Ph), 139.31 (s, $C^{29,47}$), 138.93 (s, *ipso*-Ph), 133.51 (d, $^{2}J_{P,C}$ 10 Hz, *o*-Ph), 133.31 (d, $^{2}J_{P,C}$ 10 Hz, *o*-Ph), 132.05 (s, *p*-Ph), 131.75 (s, *p*-Ph), 130.84 (s, $C^{10,13}$), 130.28 (dd, $^{2}J_{Y,C,}$ $^{2}J_{P,C,}$ 25 Hz, 80 Hz, $C^{4,5}$), 129.04 (s, $CH^{26,44}$), 128.96 (s, *m*-Ph), 128.86 (s, $CH^{28,46}$), 128.79 (s, *m*-Ph), 124.87 (d, $^{3}J_{P,C}$ 16 Hz, $CH^{27,45}$), 117.78 (d, $^{3}J_{P,C}$ 11 Hz, $CH^{3,6}$), 111.86 (s, $CH^{1,8}$), 35.37 (s, CMe_2), 35.31, 28.13 (2 × s, CMe_2), 34.63 (s, CMe_3), 34.68 (d, $^{1}J_{Y,C}$ 37 Hz, CH_2SiMe_3), 31.47 (s, CMe_3), 4.75 (s, CH_2SiMe_3) ppm. **$^{31}P\{^{1}H\}$ NMR (C_6D_6, 243 MHz, 298K):** δ 28.85 (d, $^{2}J_{Y,P}$ 11.4 Hz). **$C_{63}H_{67}O_1N_2P_2SiY$ (1047.16 g mol^{-1}):** calcd. C 72.26, H 6.45, 2.68; found C 71.79, H 6.80, N 2.61. X-ray quality crystals of $[(\{Ph_2(C_6H_4)PN\}_2XT)Y(CH_2SiMe_3)(THF)]\cdot 2THF$ (**1-THF**·2THF) were grown by layering hexanes onto a saturated solution of **1** in THF, and cooling to –28 °C.

4.5 Synthesis of [($\{Ph_2(C_6H_4)PN\}_2$NAP)Y(CH_2SiMe_3)(THF)] (2-THF): A solution of $(Ph_3PN)_2NAP$ (124 mg, 0.18 mmol) in toluene (15 mL) was added dropwise to a solution of $[Y(CH_2SiMe_3)_3(THF)_2]$ (100 mg, 0.20 mmol) in toluene (10 mL) at room temperature. The reaction was stirred for 1 hour and then the solvent was removed in vacuo to afford an off white solid. This solid was then washed with hexanes (3 × ~2 mL), and then dried under vacuum for 4 hours, yielding **2-THF** as an off white solid (121 mg, 72.6%). **^{1}H NMR (C_6D_6, 600 MHz, 298K):** δ 8.52 (d, 2H, $^{3}J_{H,H}$ 7 Hz , $CH^{18,30}$), 7.74-7.71 (m, 4H, *o*-Ph), 7.48-7.45 (m, 4H, *o*-Ph), 7.30-7.28 (m, 2H, $CH^{19,31}$), 7.14 (d, 2H, $^{3}J_{H,H}$ 8 Hz, $CH^{4,5}$), 7.07-7.03 (m, 2H, $CH^{21,33}$), 6.99-6.96 (broad m, 2H, *p*-Ph), 6.99-6.96 (br m, 4H, *m*-Ph), 6.96-6.93 (m, 2H, $CH^{2,7}$), 6.96-6.93 (m, 2H, $CH^{20,32}$), 6.92-6.88 (m, 2H, *p*-Ph), 6.83 (appt. t, 2H, $^{3}J_{H,H}$ 8 Hz, $^{3}J_{H,H}$ 8 Hz, $CH^{3,6}$), 6.72-6.69 (m, 4H, *m*-Ph), 3.67 (m, 4H, THF), 1.22 (m, 4H, THF), 0.41 (s, 9H, CH_2SiMe_3), –0.15 (d, 2H, $^{2}J_{Y,H}$ 2 Hz, CH_2SiMe_3) ppm. **$^{13}C\{^{1}H\}$ NMR (C_6D_6, 151 MHz, 298K):** δ 197.52 (app. t, *J* 42 Hz, $C^{17,29}$), 145.26 (d, $^{2}J_{P,C}$ 6 Hz, $C^{1,8}$), 139.48 (d, $^{2}J_{Y,C}$ 26 Hz, $CH^{18,30}$), 138.50 (app. t, *J* 70 Hz, $C^{22,34}$), 133.61 (d, $^{2}J_{P,C}$ 9 Hz, *o*-Ph), 133.49 (d, $^{2}J_{P,C}$ 9 Hz, *o*-Ph), 133.23 (s, *ipso*-Ph), 132.71 (s, *ipso*-Ph), 131.54 (s, *p*-Ph), 131.23 (s, *p*-Ph), 130.30, 129.76 (2 × s, C^{9} and C^{10}), 129.34 (s, $CH^{19,31}$), 129.13 (d, $^{2}J_{P,C}$ 4 Hz, $CH^{21,33}$), 128.78 (d, $^{3}J_{P,C}$ 11 Hz, *m*-Ph), 128.43 (d, $^{3}J_{P,C}$ 11 Hz, *m*-Ph), 125.35 (d, $^{3}J_{P,C}$ 16 Hz, $CH^{20,32}$), 125.04 (s, $CH^{3,6}$), 122.29 (s, $CH^{4,5}$), 121.38 (d, $^{3}J_{P,C}$ 13 Hz, $CH^{2,7}$), 69.05 (s, THF), 25.33 (s, THF), 30.82 (d, $^{1}J_{Y,C}$ 34 Hz, CH_2SiMe_3), 5.02 (s, CH_2SiMe_3) ppm. **$^{31}P\{^{1}H\}$ NMR (C_6D_6, 243 MHz, 298K):** δ 28.49 (d, $^{2}J_{Y,P}$ 12 Hz) ppm. **$C_{54}H_{53}ON_2P_2SiY$ (924.95 g mol^{-1}):** calcd. C 70.12, H 5.78, N 3.03 %; found C 69.31, H 5.79, N 2.58 % (some thermal decomposition likely occurred during transport to Indianapolis for elemental analysis). X-ray quality crystals of $[(\{Ph_2(C_6H_4)PN\}_2NAP)Y(CH_2SiMe_3)(DME)\cdot hexane]$ (**2-DME**·hexane) were grown by layering a saturated solution of **1** in DME with hexanes, followed by cooling to –28 °C.

Acknowledgement

This research was supported by the Natural Sciences and Engineering Research Council (NSERC) of Canada via a Discovery Grant.

Supplementary Data

Supplementary Data for this article (NMR spectra) can be found at xxxxxxxxxxxxxx. CCDC 1953372-1953373 contain the crystallographic data for compounds **1-THF** and **2-DME**, respectively.

References

1 (a) F.T. Edelmann, D.M.M. Freckmann, H. Schumann, Chem. Rev. 102 (2002) 1851-1896; (b) W.E. Piers, D.J.H. Emslie, Coord. Chem. Rev. 233 (2002) 131-155; (c) P.M. Zeimentz, S. Arndt, B.R. Elvidge, J. Okuda, Chem. Rev. 106 (2006) 2404-2433; (d) M. Konkol, J. Okuda, Coord. Chem. Rev. 252 (2008) 1577-1591; (e) A.A. Trifonov, Coord. Chem. Rev. 254 (2010) 1327-1347; (f) M. Nishiura, Z.M. Hou, Nat. Chem. 2 (2010) 257-268; (g) F.T. Edelmann, Chem. Soc. Rev. 41 (2012) 7657-7672; (h) T.S. Li, S. Kaercher, P.W. Roesky, Chem. Soc. Rev. 43 (2014) 42-57; (i) P.L. Arnold, M.W. McMullon, J. Rieb, F.E. Kuhn, Angew. Chem. Int. Ed. 54 (2015) 82-100; (j) W.Q. Mao, L. Xiang, Y.F. Chen, Coord. Chem. Rev. 346 (2017) 77-90; (k) J. Okuda, Coord. Chem. Rev. 340 (2017) 2-9; (l) A.A. Trifonov, D.M. Lyubov, Coord. Chem. Rev. 340 (2017) 10-61.

2 (a) C.A. Cruz, D.J.H. Emslie, H.A. Jenkins, J.F. Britten, Dalton Trans. 39 (2010) 6626-6628; (b) N.R. Andreychuk, D.J.H. Emslie, H.A. Jenkins, J.F. Britten, J. Organomet. Chem. 857 (2018) 16-24; (c) N.R. Andreychuk, S. Ilango, B. Vidjayacoumar, D.J.H. Emslie, H.A. Jenkins, Organometallics 32 (2013) 1466-1474.

3 C.A. Cruz, D.J.H. Emslie, L.E. Harrington, J.F. Britten, Organometallics 27 (2008) 15-17.

4 C.A. Cruz, D.J.H. Emslie, L.E. Harrington, J.F. Britten, C.M. Robertson, Organometallics 26 (2007) 692-701.

5 C.A. Cruz, D.J.H. Emslie, C.M. Robertson, L.E. Harrington, H.A. Jenkins, J.F. Britten, Organometallics 28 (2009) 1891-1899.

6 K.S.A. Motolko, D.J.H. Emslie, J.F. Britten, RSC Adv. 7 (2017) 27938-27945.

7 K.S.A. Motolko, D.J.H. Emslie, H.A. Jenkins, Organometallics 36 (2017) 1601-1608.

8 (a) N.K. Hangaly, A.R. Petrov, M. Elfferding, K. Harms, J. Sundermeyer, Dalton Trans. 43 (2014) 7109-7120; (b) Z. Jian, N.K. Hangaly, W. Rong, Z. Mou, D. Liu, S. Li, A.A. Trifonov, J. Sundermeyer, D. Cui, Organometallics 31 (2012) 4579-4587; (c) K.A. Rufanov, A.R. Petrov, V.V. Kotov, F. Laquai, J. Sundermeyer, Eur. J. Inorg. Chem. 2005 (2005) 3805-3807.

9 (a) N.K. Hangaly, A.R. Petrov, K.A. Rufanov, K. Harms, M. Elfferding, J. Sundermeyer, Organometallics 30 (2011) 4544-4554; (b) Z. Jian, A.R. Petrov, N.K. Hangaly, S. Li, W. Rong, Z. Mou, K.A. Rufanov, K. Harms, J. Sundermeyer, D. Cui, Organometallics 31 (2012) 4267-4282.

10 N.S. Hillesheim, M. Elfferding, T. Linder, J. Sundermeyer, Z. Anorg. Allg. Chem. 636 (2010) 1776-1782.

11 W.F. Rong, D.T. Liu, H.P. Zuo, Y.P. Pan, Z.B. Jian, S.H. Li, D.M. Cui, Organometallics 32 (2013) 1166-1175.

12 (a) D. Li, S. Li, D. Cui, X. Zhang, J. Organomet. Chem. 695 (2010) 2781-2788; (b) D. Li, S. Li, D. Cui, X. Zhang, A.A. Trifonov, Dalton Trans. 40 (2011) 2151-2153; (c) H. Xie, X. Hua, B. Liu, C. Wu, D. Cui, J. Organomet. Chem. 798 (2015) 335-340.

13 K.D. Conroy, W.E. Piers, M. Parvez, J. Organomet. Chem. 693 (2008) 834-846.

14 (a) B. Liu, D. Cui, J. Ma, X. Chen, X. Jing, Chem. Eur. J. 13 (2007) 834-845; (b) B. Liu, X. Liu, D. Cui, L. Liu, Organometallics 28 (2009) 1453-1460.

15 D. Wang, S.H. Li, X.L. Liu, W. Gao, D.M. Cui, Organometallics 27 (2008) 6531-6538.

16 N.Y. Rad'kova, A.O. Tolpygin, V.Y. Rad'kov, N.M. Khamaletdinova, A.V. Cherkasov, G.K. Fukin, A.A. Trifonov, Dalton Trans. 45 (2016) 18572-18584.

17 J.L. Brosmer, P.L. Diaconescu, Organometallics 34 (2015) 2567-2572.

18 Z.C. Zhang, D.M. Cui, Chem. Eur. J 17 (2011) 11520-11526.

19 (a) K.R. Johnson, P.G. Hayes, Dalton Trans. 43 (2014) 2448-2457; (b) K.R.D. Johnson, P.G. Hayes, Organometallics 30 (2011) 58-67; (c) K.R.D. Johnson, B.L. Kamenz, P.G. Hayes, Can. J. Chem 94 (2016) 330-341.

20 K.R.D. Johnson, P.G. Hayes, Organometallics 28 (2009) 6352-6361.

21 K.R.D. Johnson, P.G. Hayes, Organometallics 32 (2013) 4046-4049.22 K.R.D. Johnson, P.G. Hayes, Inorg. Chim. Acta 422 (2014) 209-217.

23 (a) K.R. Johnson, M.A. Hannon, J.S. Ritch, P.G. Hayes, Dalton Trans. 41 (2012) 7873-7875; (b) M.T. Zamora, K.R. Johnson, M.M. Hanninen, P.G. Hayes, Dalton Trans. 43 (2014) 10739-10750.

24 (a) E.L. Lu, W. Gan, Y.F. Chen, Dalton Trans. 40 (2011) 2366-2374; (b) P.L. Watson, Chem. Commun. (1983) 276-277; (c) A.L. Wayda, J.L. Atwood, W.E. Hunter, Organometallics 3 (1984) 939-941; (d) P.M. Zeimentz, J. Okuda, Organometallics 26 (2007) 6388-6396.

25 (a) M. Brookhart, M.L.H. Green, J. Organomet. Chem. 250 (1983) 395-408; (b) K.H. Denhaan, J.L. Deboer, J.H. Teuben, A.L. Spek, B. Kojicprodic, G.R. Hays, R. Huis, Organometallics 5 (1986) 1726-1733; (c) D.A. Pantazis, J.E. McGrady, M. Besora, F. Maseras, M. Etienne, Organometallics 27 (2008) 1128-1134; (d) A.F. Dunlop-Briere, P.H.M. Budzelaar, M.C. Baird, Organometallics 31 (2012) 1591-1594.

26 (a) N.R. Andreychuk, T. Dickie, D.J.H. Emslie, H.A. Jenkins, Dalton Trans. 47 (2018) 4866-4876; (b) K.S.A. Motolko, D.J.H. Emslie, H.A. Jenkins, J.F. Britten, Eur. J. Inorg. Chem. (2017) 2920-2927; (c) K.S.A. Motolko, J.S. Price, D.J.H. Emslie, H.A. Jenkins, J.F. Britten, Organometallics 36 (2017) 3084-3093; (d) B. Vidjayacoumar, S. Ilango, M.J. Ray, T. Chu, K.B. Kolpin, N.R. Andreychuk, C.A. Cruz, D.J.H. Emslie, H.A. Jenkins, J.F. Britten, Dalton Trans. 41 (2012) 8175-8189.

27 C.A. Cruz, T. Chu, D.J.H. Emslie, H.A. Jenkins, L.E. Harrington, J.F. Britten, J. Organomet. Chem. 695 (2010) 2798-2803.

28 Based on a search of the Cambridge Structural Database conducted in September 2019. C. R. Groom, I. J. Bruno, M. P. Lightfoot and S. C. Ward, Acta Cryst. (2016). B72, 171-179.

29 S. Bambirra, S.J. Boot, D. van Leusen, A. Meetsma, B. Hessen, Organometallics 23 (2004) 1891-1898.

30 S. Bambirra, A. Meetsma, B. Hessen, A.P. Bruins, Organometallics 25 (2006) 3486-3495.

31 D.M. Lyubov, A.V. Cherkasov, G.K. Fukin, A.A. Trifonov, Organometallics 35 (2016) 126-137.

32 (a) Resanovic, S. Chromium and Neodymium Complexes of bis-Phosphinimine Pincer Ligands and Their Behaviour in 1,3-Butadiene Polymerization. Chemistry, Masters Thesis, University of Toronto: Toronto, ON, 2011; (b) S. Bradbury, C.W. Rees, R.C. Storr, J. Chem. Soc., Perkin Trans 1 (1972) 68-71.

33 Simple alkyl diaryl lanthanide complexes have recently received attention as reagents, (generated in situ by rare earth–halogen exchange) for subsequent reaction with organic electrophiles: (a) L. Anthore-Dalion, A.D. Benischke, B. Wei, G. Berionni, P. Knochel, Angew. Chem. Int. Ed 58 (2019) 4046-4050; (b) A.D. Benischke, L. Anthore-Dalion, G. Berionni, P. Knochel, Angew. Chem. Int. Ed 56 (2017) 16390-16394; (c) A.D. Benischke, L. Anthore-Dalion, F. Kohl, P. Knochel, Chem. Eur. J. 24 (2018) 11103-11109.

34 J.S. Nowick, P. Ballester, F. Ebmeyer, J. Rebek, J. Am. Chem. Soc. 112 (1990) 8902-8906.

35 F. Estler, G. Eickerling, E. Herdtweck, R. Anwander, Organometallics 22 (2003) 1212-1222.

36 A. Pollex, M. Hiersemann, Org. Lett. 7 (2005) 5705-5708.

37 A.F. Burchat, J.M. Chong, N. Nielsen, J. Organomet. Chem 542 (1997) 281-283.

38 Dolomanov, O.V., Bourhis, L.J., Gildea, R.J, Howard, J.A.K. & Puschmann, H. (2009), J. Appl. Cryst. 42, 339-341.

39 G.M. Sheldrick, Acta Crystallogr. Sect. A 71 (2015) 3-8.

40 Sheldrick, G. M. (2008). Acta Cryst. A64, 112-122.